EVALUATION OF PARAMETERS OF CAVITATIONAL FLOW IN HYDRAULIC SYSTEMS

G. S. Nazarov

UDC 532.555:532.528

The possibility of application of the Borda–Carnot theorems by evaluating parameters of cavitational flow in hydraulic systems is considered. Experimental data for different channels of various forms are obtained and a description is given of processes which take place at different points in the channel.

Cavitational flow is characterized by the appearance of a vapor phase on the channel boundaries and by establishment of constant pressure at the points of flow separation. In individual cases this leads to limitation of the discharge of the liquid, and to the appearance of what are known as "plateaux" of constant discharge on the characteristics of the hydraulic systems. Flow around surfaces of marked curvature with change of channel section is accompanied by curving of the lines of flow and generation of local contractions with subsequent expansion of the flow, as a result of which at the end of the zone of separation losses of full pressure occur which are determined by the Borda–Carnot theorem.

Let us consider the problem of distribution of energy over individual parts of a nonclosed hydraulic system, which consists of K series connected stages. Each stage consists of three parts: inlet, working section, and outlet. Outlet from the first stage forms the inlet of the second stage, etc. In the working parts energy is supplied to the liquid flow resulting in increase of the total pressure in the hydraulic system (the process proceeds adiabatically). We will designate the working parts with odd numbers 1, 3, 5, 7, . . . , n – 1, where n = 2 K. The inlet and outlet parts are numbered with even numbers 0, 2, 4, . . . , n. In the parts (1-2), (3-4), (5-6), . . . ,[(n – 1) – n] occur losses of total pressure which are associated with the sudden expansion of the flow.

The equations

$$\begin{aligned} \Delta p_1^* &= p_1^* - p_0^*, \\ \Delta p_3^* &= p_3^* - p_2^*, \\ &\cdots\cdots\cdots \\ \Delta p_{n-1}^* &= p_{n-1}^* - p_{n-2}^* \end{aligned} \tag{1}$$

characterize energy supplied to the stages. According to the Borda–Carnot theorem for the first stage we have

$$p_1^* - p_2^* = \frac{\rho}{2}(c_1 - c_2)^2. \tag{2}$$

On eliminating by means of the Bernoulli equations p_1^* and p_2^* from (1) and (2):

$$c_1^2 = \frac{p_0^* - p_1 + \Delta p_1^*}{\frac{\rho}{2}}, \tag{3}$$

$$c_1 = \frac{\rho c_2^2 + (p_2 - p_1)}{\rho c_2}. \tag{4}$$

P. I. Baranov Central Institute of Aviation Engine Construction, Moscow. Translated from Inzhenerno-Fizicheskii Zhurnal, Vol. 17, No. 3, pp. 397-406, September, 1969. Original article submitted February 4, 1968.

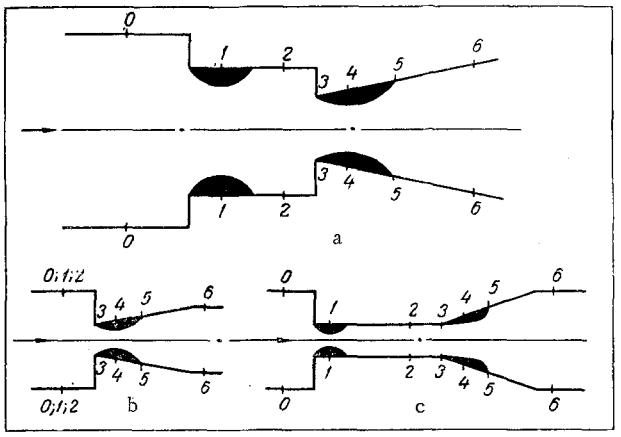

Fig. 1

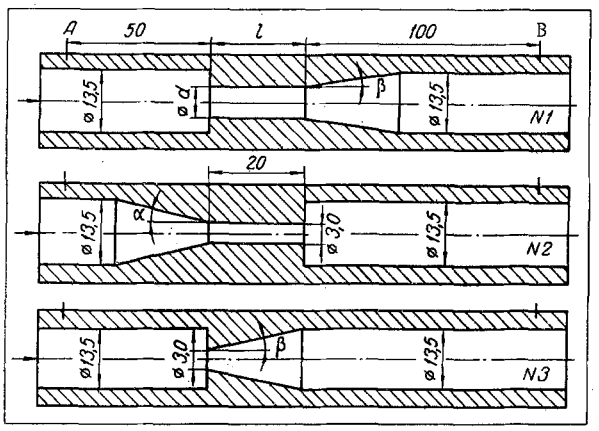

Fig. 2

Fig. 1. Diagram of liquid flow in two-stage channels of different types (the figures indicate the characteristic cross sections of the channels): a) channel of general type. The areas of the cross sections (0–0)-(6–6) are different: 0–0) wide section with inlet to the channel; 1–1) contraction of flow with flow round the inlet edge of the cylindrical part; 2–2) cross section of the channel at the point of reattachment of the zone of separation of flow in the cylindrical part; 3–3) minimum cross section of diffusor; 4–4) contraction of the flow with flow round the inlet edge of the diffuser; 6–6) wide cross section at the outlet from the channel, where the fields of speeds and full pressures are levelled out; b) channel without a cylindrical part at the contracting point, has similar cross-section areas (0–0), (1–1), and (2–2); c) channel with a cylindrical part at the contracting point, has similar cross-section areas (2–2) and (3–3).

Fig. 2. Basic dimensions and form of the channels (liquid flow from left to right). The number indicates the type of the channel. Channels No. 1 are distinguished by the diameter d in the narrowest section, by length l of the cylindrical parts and by the outlet angles β = 5 to 90°. Channels No. 2 are distinguished by the inlet angles α = 30 to 90°. Channels No. 3 do not have cylindrical parts at the contraction. They are distinguished by the outlet angles of β = 5 to 12°. Static pressure was measured at points A and B.

We will square (4) and equate to (3). After transformation we will obtain

$$p_2^* = p_0^* + \Delta p_1^* - \frac{(p_2 - p_1)^2}{4\frac{\rho}{2}c_2^2}. \tag{5}$$

We will write analogous equations for each of the K stages

$$\left.\begin{aligned} p_2^* &= p_0^* + \Delta p_1^* - \frac{(p_2 - p_1)^2}{4\frac{\rho}{2}c_2^2} \\ p_4^* &= p_2^* + \Delta p_3^* - \frac{(p_4 - p_3)^2}{4\frac{\rho}{2}c_4^2} \\ &\cdots\cdots\cdots\cdots\cdots \\ p_n^* &= p_{n-2}^* + \Delta p_{n-1}^* - \frac{(p_n - p_{n-1})^2}{4\frac{\rho}{2}c_n^2} \end{aligned}\right\}. \tag{6}$$

After elimination of intermediate p* values (2, 4, 6, . . . , n – 2) from the system of equations (6) and on dividing by γ we obtain a characteristic equation of distribution of energy in the different parts of the hydraulic system

$$\frac{p_n^* - p_0^*}{\gamma} = H_1 + H_3 + \ldots + H_{n-1} - \left[\frac{\left(\frac{p_2 - p_1}{\gamma}\right)^2}{4\frac{c_2^2}{2g}} + \frac{\left(\frac{p_4 - p_3}{\gamma}\right)^2}{4\frac{c_4^2}{2g}} + \ldots + \frac{\left(\frac{p_n - p_{n-1}}{\gamma}\right)^2}{4\frac{c_n^2}{2g}}\right], \tag{7}$$

where $H = \Delta p^*/\gamma$.

We will examine the part of the hydraulic system where there is no supply of energy ($H_1 + H_3 + H_5 + \ldots + H_{n-1} = 0$).

In the case of liquid flow with separation of the flow from the edges of the two-stage channel (Fig. 1a) the losses of full pressure in the stages are determined by the equations:

$$\frac{(p_2 - p_1)^2}{p_0^* - p_2^*} = 4\frac{\rho}{2}c_2^2, \tag{8}$$

$$\frac{(p_5 - p_4)^2}{p_3^* - p_5^*} = 4\frac{\rho}{2}c_5^2. \tag{9}$$

With the condition

$$p_2^* = p_3^*, \quad p_5^* = p_6^*$$

or

$$p_2 = p_3^* - \frac{\rho}{2}c_2^2, \quad p_5 = p_6^* - \frac{\rho}{2}c_5^2$$

we will obtain:

$$\left(p_3^* - p_1 - \frac{\rho}{2}c_2^2\right)^2 = 4\frac{\rho}{2}c_2^2(p_0^* - p_3^*), \tag{10}$$

$$\left(p_6^* - p_4 - \frac{\rho}{2}c_5^2\right)^2 = 4\frac{\rho}{2}c_5^2(p_3^* - p_6^*). \tag{11}$$

We will solve (10), and (11) for p_3^* and we will compare

$$p_6^* - \left(p_4 + \frac{\rho}{2}c_5^2\right) = 2\sqrt{\frac{\rho}{2}c_5^2\left[p_1 - \frac{\rho}{2}c_2^2 \pm \sqrt{4\frac{\rho}{2}c_2^2(p_0^* - p_1) - p_6^*}\right]}.$$

We express c_2 by c_3 by means of the equation of continuity where c_3 is the speed in the narrowest section of the channel and we solve the obtained expression for c_5 which is the speed of the jet at the end of the expanding section. After dividing by c_3 we obtain a formula for determining the magnitude of the relative speed of the jet $\bar{C} = c_5/c_3$:

$$\bar{C} = \sqrt{2\frac{F_3}{F_2}\sqrt{\frac{p_0^* - p_1}{\frac{\rho}{2}c_3^2} - \left(\frac{F_3}{F_2}\right)^2} - \frac{p_4 - p_1}{\frac{\rho}{2}c_3^2}} - \sqrt{2\frac{F_3}{F_2}\sqrt{\frac{p_0^* - p_1}{\frac{\rho}{2}c_3^2} - \left(\frac{F_3}{F_2}\right)^2} - \frac{p_6^* - p_1}{\frac{\rho}{2}c_3^2}}. \tag{12}$$

Two particular cases are of special interest:

1) $F_2 \gg F_3$ (Fig. 1b), where $F_3/F_2 \to 0$, $p_1 \approx p_0^*$ and

$$\bar{C} = \sqrt{\frac{p_0^* - p_4}{\frac{\rho}{2}c_3^2}} - \sqrt{\frac{p_0^* - p_6^*}{\frac{\rho}{2}c_3^2}}; \tag{13}$$

2) $F_2 = F_3$ (Fig. 1c), where formula (12) assumes the form

$$\bar{C} = \sqrt{2\sqrt{\frac{p_0^* - p_1}{\frac{\rho}{2}c_3^2}} - \frac{p_4 - p_1}{\frac{\rho}{2}c_3^2} - 1} - \sqrt{2\sqrt{\frac{p_0^* - p_1}{\frac{\rho}{2}c_3^2}} - \frac{p_6^* - p_1}{\frac{\rho}{2}c_3^2} - 1}. \tag{14}$$

In the formulas (12), (13), and (14) p_1 and p_4 are static pressures at the flow contractions in all flow regimes. Appearance of the vapor phase in the case of cavitation in the flow separation zones establishes

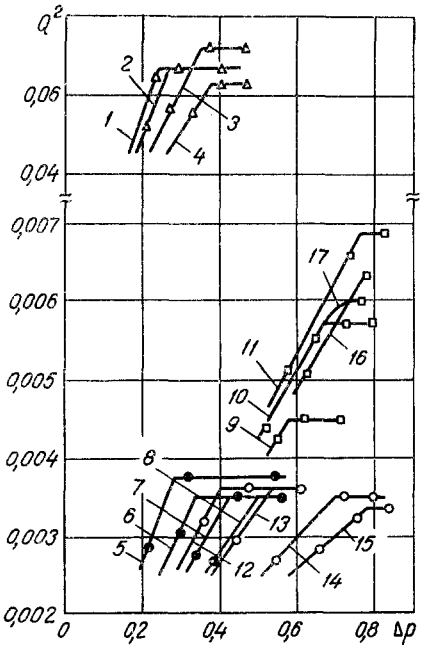

Fig. 3. Cavitation characteristics of channels of different shape in water where t = 20°C and p^*_{in} = 0.85 kg/cm^2 – the discharge Q (liters/sec) and pressure drop Δp (kg cm^2) (the black points correspond with the channels No. 1, d = 3.0 mm; the unfilled points correspond with the remainder): 1-8 channel No. 1; 1) d = 6.0 mm; l = 30 mm; β = 5°; 2) 6.0, 3.0, 7; 3) 6.0, 30, 12; 4) 6.0, 30, 20, 30, 45, 60, 75, 90; 5) 3.0, 20, 5; 6) 3.0, 20, 7; 7) 3.0, 20, 12; 8) 3.0, 20, 20, 30, 45, 60, 75, 90; 9-11 channel No. 2; 9) d = 3.0 mm, l = 20 mm, α = 60°; 10) 3.0, 20, 45; 11) 3.0, 20, 30; 12-15) channel No. 3; 12) d = 3.0 mm, l = 0, β = 5; 13) 3.0, 0, 7; 14) 3.0, 0, 10; 15) 3.0, 0, 12; 16-17) channel No. 2; 16) d = 3.0 mm; l = 20 mm, α = 45° (fluoroplastic); 7) 3.0, 20, 45 (standing water).

static pressure of the liquid at the given point in the channel which becomes equal to the sum of the pressures of saturated vapor and partial pressure of the gas within the cavitational void, i.e.,

$$p_1 = p_v + p_g, \tag{15}$$

$$p_4 = p_v + p_g, \tag{16}$$

on neglecting the surface tension force.

In the given work experimental investigation was also carried out on the cavitational characteristics of the channels of different shapes. The objects of the investigations were channels which were made from Plexiglas distinguished by the angles at the inlet, and the outlet or by diameters of the cylindrical parts of the channel at the contraction (Fig. 2). By measuring the static pressure at the inlet and outlet by using differential mercury pressure gages, before, and after a local contraction, and also the discharge, the outlet characteristics were recorded for water at a temperature of t = 20°C, taken from the water conduit directly before the experiment. The characteristics were recorded for steady pressure at the inlet which was equal to atmospheric pressure. At the outlet from the channel a rarefaction was created by means of a vacuum pump. Figure 3 shows experimental graphs constructed in the form of a relationship between the pressure drop and square of the flow rate for channels with different diameters of the local contractions and the angles at the inlet and outlet. Graphs 1-8 refer to channels of the type 1 (Fig. 2) which are distinguished by the diameters of the cylindrical parts at the contraction and by the angles β at the outlet. The graphs 9-11 refer to channels of the type 2 with different angles α at the inlet. Graphs 12-15 are obtained for channels of the type 3 without cylindrical parts at the contraction. As shown by the experiments with water, the flow parameters in the regime where the vapor phase appears on the channel edges do not vary by increasing the angle $\beta > 15°$. This led to the fact that the graphs of the characteristics of the channels with angles β = 20, 30, 45, 60, 75, 90° are on top of each other and therefore in Fig. 3 for each value of the diameter d they are given by a single relationship (4, 8).

Visual observations of the flow in transparent channels and photography of the processes showed that initially the "plateau" of the characteristics (at constant discharge) corresponds to the moment of formation, on the channel edge section of parts of free surface of the liquid in one of the zones of flow separation. It is known that an important part in the cavitational processes is played by the wetting of the channel walls [1]. The effect of wetting is especially manifested in the case of slight pressure drops. The susceptibility to cavitation of the liquid is also of considerable importance. Figure 3 shows among others the characteristics for channels of uniform profile (No. 2, α = 45°) which are made from fluoroplastics and from Plexiglas of which the wetting properties of the former are not as good as those of the latter. The graph shows that the characteristic of the channel made from fluoroplastics (relation 16) does not have a "plateau" while the characteristic of a similar channel made from Plexiglas (relation 10) has the "plateau"

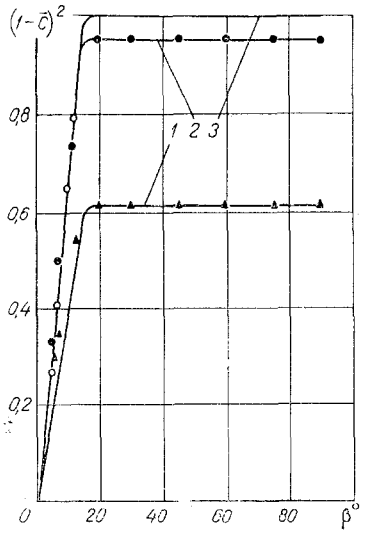

Fig. 4. Generalized graph for parameters of cavitation flow in channels of different shape (the nonfilled points refer to channels No. 3; the black ones refer to channels No. 1: 1) d/D = 0.44; 2) d/D = 0.22; 3) d/D → 0.

TABLE 1. Values of the Coefficient of Contraction of the Stream for Channels No. 2

α°	φ	α°	φ
30	0,87	60	0,69
45	0,78	90	0,65

at constant discharge. However, on investigating this channel with water which had been standing in an open vessel for some days, the discharge was changed monotonically and it reached a maximum value on the appearance of the cavitation on the outlet edge of the channel (relation 17). As a result of settling, mechanical admixtures, which had precipitated to the bottom, and also air bubbles in the nondissolved state could be removed from the water which acquired the property of withstanding tensile stresses, as a result of which the appearance of cavitation on the inlet edge was delayed. With further decrease of pressure in the outlet, at a given moment of time, bubble-type cavitation occurred on the inlet edge of the channel, and parts of free surface of the liquid appeared. The discharge then decreased in jumps to a magnitude corresponding to the value of the "plateau" obtained earlier in an experiment with water taken from the water pipe directly before the experiment (relation 10), and it remained constant up to a condition of full separation of the flow with formation of a free stream in the outlet.

In accordance with what we have examined, the parameters of flow in the conditions of the beginning of cavitation in channels without cylindrical parts at the contraction are determined by Eq. (13). The flow parameters in the condition of occurrence of cavitation at the inlet edges of channels with cylindrical parts at the contraction are determined by Eq. (14). The smallest cross section in which the vapor phase is formed and the minimum pressure is established is the cross section 1–1 (Fig. 1c). We will therefore exclude the parameter p_4 from Eq. (14). Adopting the relationships:

$$p_4^* - p_5^* = \frac{\rho}{2}(c_4 - c_5)^2;$$

$$p_4^* = p_4 + \frac{\rho}{2}c_4^2;$$

$$p_5^* = p_6^*$$

and expressing c_4 through c_3 by means of the equation of continuity, and taking account of the fact that in the case of flow of liquid at the point at which the cylindrical part changes into a conical part (Fig. 1c) there is no contraction of the flow ($F_3 = F_4$), we will obtain

$$(1-\bar{C})^2 = 2\sqrt{\frac{p_0^* - p_1}{\frac{\rho}{2}c_3^2} - \frac{p_6^* - p_1}{\frac{\rho}{2}c_3^2}} - 1. \tag{17}$$

Substituting (15), and (16) into (13), and (17), we will write

$$\bar{C} = \sqrt{\frac{p_0^* - (p_v + p_g)}{\frac{\rho}{2}c_3^2}} - \sqrt{\frac{p_0^* - p_6^*}{\frac{\rho}{2}c_3^2}}, \tag{18}$$

$$(1-\bar{C})^2 = 2\sqrt{\frac{p_0^* - (p_v + p_g)}{\frac{\rho}{2}c_3^2} - \frac{p_6^* - (p_v + p_g)}{\frac{\rho}{2}c_3^2}} - 1. \tag{19}$$

The formulas (18) and (19) determine the instant at which the vapor phase occurs on the edges of the channel in relation to the parameters of the flow, and the speed of flow at the end of the separation zone. In these relationships the first term of the right-hand side is expressed by the coefficient of contraction of the free stream when a cavitation zone is formed at the outlet of the channel [2]

$$\varphi = \frac{1}{\sqrt{\dfrac{p_0^* - (p_v + p_g)}{\dfrac{\rho}{2} c_3^2}}}. \tag{20}$$

Since the discharge did not change, the coefficient φ is related to all the "plateau" conditions of the characteristics $Q^2 = f(\Delta p)$, observed in the case of constant pressure at the inlet.

By using the formulas obtained, the experimental data for channels of all types were obtained (Fig. 2). The calculation was carried out according to the parameters of the last point of the sloping part of each of the characteristics $Q^2 = f(\Delta p)$, represented in Fig. 3. This point corresponds with the instant of occurrence of a vapor phase in the flow separation zones on the edges of the channel at the contraction. By using formula (18), the characteristics of the channels without cylindrical parts in the contraction are treated. By using formula (19) the characteristics of the channels with cylindrical parts in the contraction are calculated. The values of the contraction coefficient φ were determined according to formula (20) for cavitation systems with formation of a free stream at the outlet. The pressure $p_v + p_g$ at the place where cavitation occurs for water where $t = 20°C$, as the measurements showed was small and in the calculations it was taken to be zero. In the case of treatment of the characteristics of the channels with cylindrical parts, a correction was introduced to the losses of full pressure due to friction along the length of these parts. The calculated magnitude p_6^* was taken as the sum of the measured static pressure of the dynamic pressure in the tube at the outlet and the losses calculated according to the Darcy–Weisbach formula for circular channels $\delta p^* = \eta(L/d)(\rho/2)c_3^2$, where η is the coefficient of hydraulic resistance depending on the Re number (in this case Re = 25,000-50,000).

The results of the treatment are given in Fig. 4 and in Table 1. The graph shows that the magnitude $(1 - \overline{C})^2$, which characterizes the relationship of the speeds of the flow at the end and at the beginning of expansion, is determined by the relationship of the diameters d/D and it is general for channels of different shape. In the case of $0 < \beta < 15°$ it varies in proportion to the angle at the outlet. This indicates that the zone of separation of the flow is reattached in the conical part of the channel. In the case of $\beta > 15°$ $(1 - \overline{C})^2$ differs little from $(1 - \overline{F})^2$. Consequently, in this case the zone of separation of the flow is reattached in the cylindrical tube on the outlet (the pressure p_6^* is measured in the same way). The graph in Fig. 4 shows that the magnitude $(1 - \overline{C})^2$ is determined by two geometrical parameters: the angle β on the outlet, and the relationship of the diameters d/D, but the coefficient φ (see Table 1) depends on the geometry of the channel at the inlet. It is possible to show that the experimental values of the coefficient of contraction φ in the case of formation of a free stream in the outlet, which are shown in Table 1 for channels with different angles α at the input, are close to the values calculated according to the Weisbach–Zeiner formula

$$\varphi = 0.64 + 0.212 \cos^3 \alpha + 0.106 \cos^4 \alpha, \tag{21}$$

which is obtained for discharge of liquid into the atmosphere for contracting nozzles [3].

It is useful to use the relationships given in Fig. 4 together with the formulas (19), (20), and (21), in calculation of the parameters of cavitation flow in straight channels of circular cross section, which have cylindrical parts in the contraction. The order of calculation is as follows:

1) An angle α is assigned at the inlet. The value of the coefficient φ is determined from formula (21).

2) An excess pressure is assigned at the inlet above the pressure of elasticity of saturated vapor $p_0^* - (p_v + p_g)$ and by means of substitution into Eq. (20) for the coefficient φ the dynamic pressure $(\rho/2)c_3^2$ is determined in the smallest cross section of the channel, according to the magnitude of which the discharge of liquid corresponding to the "plateau" of the characteristic is calculated.

3) The angle β is assigned at the outlet, in addition to the ratio of the diameters d/D in the smallest cross section of the channel and in the tube on the outlet. The parameter $(1 - \overline{C})^2$ is determined according to the graph of Fig. 4.

4) By substituting the found values p_0^*, $(p_V + p_g)$, $(\rho/2)c_5^2$, and $(1 - \overline{C})^2$ into formula (19) the pressure in the outlet p_6^* which corresponds to the beginning of the section of constant discharge on the cavitation characteristic is determined.

NOTATION

p^*	is the total pressure;
p	is the static pressure;
Δp^*	is the difference of total pressures;
Δp	is the difference of static pressures;
c	is the speed of flow;
ρ	is the density of the liquid;
γ	is the specific weight of the liquid;
H	is the pressure head;
F	is the area of the cross section of the channel;
$p_V + p_g$	are the sum of pressures of vapor and gas in the cavitation bubble;
α	is the angle of contraction of the channel at the inlet;
β	is the angle of expansion of the channel at the outlet;
l	is the length of the cylindrical part in the contraction;
D	is the diameter of the channel in the outlet at the point of measurement of the static pressure;
d	is the diameter of the channel at the contraction;
$\overline{C}$	is the ratio between the speeds of the flow at the end and at the beginning of the separation zone;
φ	is the coefficient of contraction of the stream;
η	is the coefficient of hydraulic resistance;
δp^*	is the magnitude of friction losses of total pressure along the length of the channel;
Re	is the Reynolds number;
$\overline{F}$	is the ratio between the areas in the smallest cross section of the channel and in the tube at the outlet.

LITERATURE CITED

1. Hall and Trister, Theoretical Foundations of Engineering Calculations [Russian translation], 88, Ser. D, No. 1, Mir, Moscow (1966).
2. G. S. Nazarov, Inzh.-Fiz. Zh., 14, No. 3 (1968).
3. A. M. Samus', Technical Hydraulics [in Russian], Gosénergoizdat, Leningrad (1933).